Journal of Nondestructive Evaluation, Vol. 12, No. 3, 1993

Crack Determination from Boundary Measurements—Reconstruction Using Experimental Data

Valdis Liepa,[1] Fadil Santosa,[2] and Michael Vogelius[3]

Received July 24, 1992; revised June 19, 1993

In this work we assess the effectiveness of Electrical Impedance Tomography for determining the presence and the location of an interior crack from boundary measurements. Electrical Impedance Tomography uses boundary voltages and currents to image the interior of a region. We collect the data needed for this nondestructive evaluation technique by laboratory experiments and apply two numerical inversion algorithms to the data. Our experiments show that the data collected are sufficient to give good estimates of crack locations and crack sizes.

KEY WORDS: Electrical impedance tomography; nondestructive evaluation; flaw imaging techniques.

1. INTRODUCTION

The goal of this work is to demonstrate that Electrical Impedance Tomography is a viable approach to crack determination. Our findings, together with those of other researchers,[2,3,6,8] lead us to conclude that this alternative procedure compares well with other more standard techniques of nondestructive testing.[10] With Electrical Impedance Tomography, one attempts to image the interior of a object by performing steady state electrical measurements on its boundary. The image produced corresponds to the conductivity distribution inside the object; the data used are current and voltage measurements.

To be precise, let us consider the following two-dimensional model problem. A circular specimen is to be inspected, the goal is to detect the presence of a single interior crack, and if a crack is present, to determine its location and size. To perform the inspection, we attach n electrodes to the surface of the specimen, as shown in Fig. 1. To generate the data needed we let steady state current in through electrode i and out through electrode

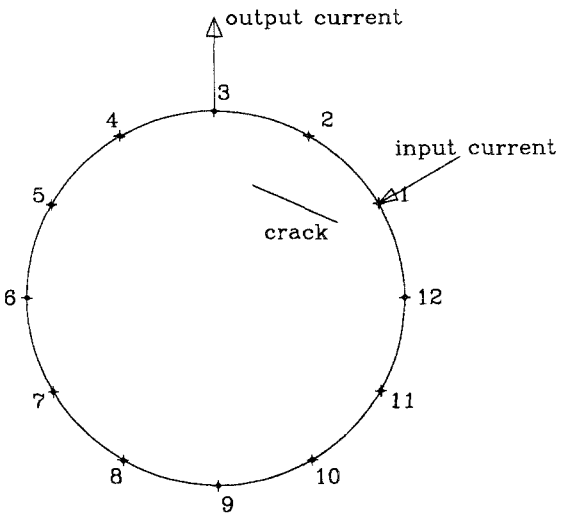

Fig. 1. A schematic diagram of the experimental setup (cross-section). The object has an interior crack, which is to be determined. A total of $n = 12$ electrodes are attached to the boundary of the object. In this example, current is flowing in at electrode $i = 1$ and out at electrode $j = 3$. Voltage drops across adjacent electrodes, $V_{k+1} - V_k$ are collected for $k = 1,\ldots,12$.

[1] Radiation Laboratory, Dept. EECS, University of Michigan, Ann Arbor, Michigan 48109.
[2] Department of Mathematical Sciences, University of Delaware, Newark, Delaware 19716.
[3] Department of Mathematics, Rutgers University, New Brunswick, New Jersey 08903.

0195-9298/93/0900-0163$07.00/0

j. Voltage drops across all adjacent pairs of electrodes are measured. Thus for a single set of measurements, the collected data consist of

1. Indices i and j
2. Current passing through i and j, I
3. Voltage drops $\triangle V_k = V_{k+1} - V_k$, for $k = 1,2,\ldots,n$.

Several different sets of measurements will be carried out to aid in the reconstruction (we know theoretically that we should perform at least two sets of measurements.[9])

In this work we will study the performance of two reconstruction algorithms. The first algorithm reconstructs a smooth conductivity distribution from the experimental data. It is based on a backprojection procedure, first developed by Barber and Brown.[2,3] The second algorithm (iteratively) reconstructs a crack in the shape of a line segment. This iterative algorithm was first developed by Santosa and Vogelius for the reconstruction of a single linear crack,[13] it has since been extended by Bryan and Vogelius to perform the reconstruction any number of linear cracks.[5] Both the backprojection algorithm and the crack finding algorithm will be described in some detail in Sections 2 and 3 of this paper.

For the first of our reconstruction algorithms we view the entire conductivity distribution inside the domain Ω as the unknown; let us denote it by $\sigma(x)$. For the second reconstruction algorithm we formally take $\sigma(x)$ of the form

$$\sigma(x) = \begin{cases} \sigma_0 & \text{if } x \in \Omega \backslash \gamma \\ \infty & \text{if } x \in \gamma \end{cases}$$

where σ_0 is known and we view the line segment $\gamma \subset \Omega$ as the unknown. The line segment γ represents a "perfectly conducting" crack. We can also treat the case of a "perfectly insulating" crack which formally corresponds to the conductivity distribution

$$\tilde{\sigma}(x) = \begin{cases} \sigma_1 & \text{if } x \in \Omega \backslash \gamma \\ 0 & \text{if } x \in \gamma \end{cases}$$

Indeed, if $\sigma_1 = 1/\sigma_0$ (in numerical value), it is very easy to see that the measured data corresponding to σ and $\tilde{\sigma}$ are related by a simple duality: the current data for $\tilde{\sigma}$ represent voltage drop data for σ, the voltage drop data for $\tilde{\sigma}$ represent current data for σ.[4]

The reconstruction algorithms will be applied to experimental data that are collected. A detailed description of the laboratory setup is given in Section 4. In a few words, the setup consists of a long cylindrical tank with 12 electrodes on its side. The electrical field in the tank is thought of as being predominantly two dimensional. To simulate cracks we immerse strips of metal vertically in the tank when filled with a homogeneous solution (water). Section 5 contains the results of application of our reconstruction methods to the experimental data.

We mention a third algorithm due to Andrieux and Ben Abda.[1] Their algorithm can be applied to locate a single linear crack (or a number of linear cracks that all lie on the same line). This novel approach is direct and very simple insofar as the location of the line is concerned. The determination of the exact location of the crack(s) on this line is still simple, but somewhat less direct, since it requires the determination of the support of a function given by an infinite series. One drawback of this algorithm is that it does not seem to have a natural extension for the reconstruction of multiple cracks that are not all lying on the same line. The direct determination of a single line, by the method of Andrieux and Ben Abda, could however form a very effective initialization step for an iterative algorithm (such as ours), even when it comes to the determination of multiple cracks. We have not so far utilized their method on data generated by our experiments. The main purpose of this paper is to demonstrate that the data collected by Impedance Imaging is sufficient in order to allow effective reconstruction. We are planning to do a comparative study of the relative effectiveness of different techniques for the crack determination problem.

2. A BACKPROJECTION IMAGING ALGORITHM

With the backprojection algorithm, we attempt to reconstruct a smoothly varying conductivity distribution $\sigma(x)$ from the boundary data. In contrast to the algorithm which will be discussed in the next section, this will not produce a line segment approximating the location of the crack. Rather, it will produce a variable conductivity distribution which has a high value for the conductivity near the crack. With this method, we can at best obtain a blurry image of the crack. However, the method is quite general and can, in principle, image more complicated internal structures.[2,3,12] Our interest in this algorithm is twofold: (1) we wish to assess the viability of such an algorithm for crack detection, and (2) since this algorithm is very efficient, we also wish to evaluate its usefulness as a tool to give a rough initial guess for the crack location.

The model equation for our problem is a divergence form elliptic equation. Let u be a steady state voltage

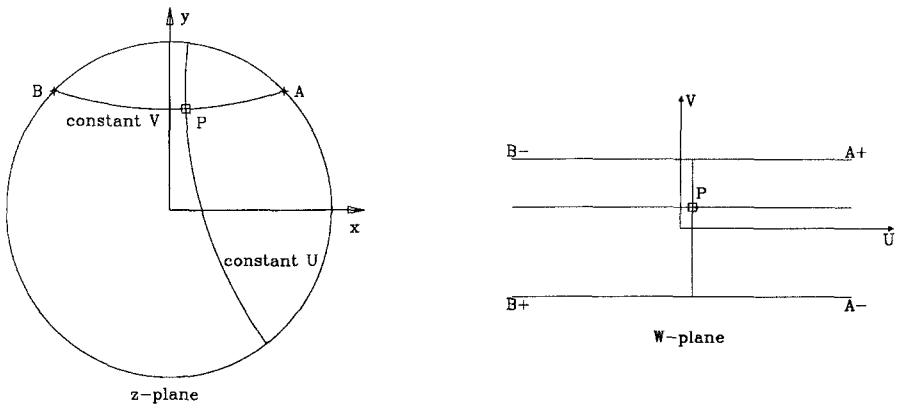

Fig. 2. A diagram describing the conformal mapping $W(\zeta(z)) = U(x,y)+\mathbf{j}V(x,y)$. The unit circle $|z| \leq 1$ is mapped to a strip $|V| \leq 1/2$. Lines of constant U in the W-plane correspond to equipotentials for the background field; lines of constant V are equi-current lines. In this diagram, current is flowing into the electrode at A and out of the electrode at B. The points A and B have been mapped to infinity as shown.

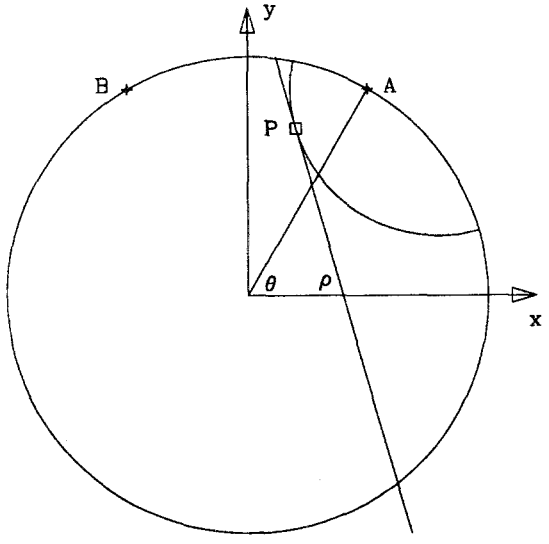

Fig. 3. Construction of the weight function $w^{(i)}(x,y)$ is illustrated in this figure. The input electrode is at A, which is at angle $\theta = \theta_i$, and the output electrode is at B. The angle between A and B is kept fixed for our data collection. To calculate the weight $w^{(i)}(x,y)$ at P, we draw the tangent to the equipotential of the background field through P at the point P. The weighting $w^{(i)}$ is $d\rho/d\theta(\theta_i)$.

potential field in the domain Ω (which here is the unit disk). Then u satisfies

$$\nabla \cdot \sigma \nabla u = 0 \text{ in } \Omega \qquad (1a)$$

The type of potential we consider here is created by letting current flow in at electrode i and out at electrode j (see Fig. 1). We refer to these two electrodes as active. Let θ_i and θ_j be the angular locations of these electrodes. The applied current is modelled by the Neumann boundary condition

$$\sigma \frac{\partial u}{\partial r}(r,\theta)\Big|_{r=1} = \chi(\theta,\theta_i) - \chi(\theta,\theta_j) \qquad (1b)$$

(in polar coordinates (r,θ)). The function $\chi(\theta,\theta_i)$ is defined to be

$$\chi(\theta,\theta_i) = \begin{cases} 1/h & \text{if } |\theta - \theta_i| \leq h/2 \\ 0 & \text{else} \end{cases}$$

so that the angular extent of the electrode is h radians. The potential, u, is unique up to a constant. To make it unique we normalize it by the requirement that

$$\int_0^{2\pi} u(1,\theta)d\theta = 0$$

Our additional data for this particular experiment consist of the voltage drops across all adjacent electrodes, i.e.,

$$u(1,\theta_{k+1}) - u(1,\theta_k) = g_k \quad \text{for} \quad k = 1,\ldots,n$$

We wish to find σ (r,θ) given such measured voltage drops for some specified choices of active electrode pairs.

We make two simplifying assumptions:

(i) the conductivity σ has the form $\sigma = 1 + \delta\sigma$ where $\delta\sigma$ is small in comparison to unity and vanishes in a neighborhood of the boundary $\{r = 1\}$;

(ii) the angular width of the electrode, h, is very small so that we may effectively model $\chi(\theta,\theta_i)$ in (1b) by a delta function.

Under these assumptions, the voltage potential u can be written in the form

$$u(r,\theta) = U(r,\theta) + \delta u(r,\theta) \quad \text{with} \quad \delta u \ll U$$

The field U will be referred to as the background field, while the field δu will be called the perturbational field. Inserting this decomposition into (1a),(1b) and collecting terms of the same order of magnitude, we obtain

$$\triangle U = 0 \qquad r < 1 \tag{2a}$$

$$\frac{\partial U}{\partial r}(1,\theta) = \delta(\theta - \theta_i) - \delta(\theta - \theta_j) \tag{2b}$$

The perturbational field δu satisfies

$$\triangle \delta u = -\nabla\, \delta\sigma \cdot \nabla U \qquad r < 1 \tag{3a}$$

$$\frac{\partial \delta u}{\partial r}(1,\theta) = 0 \tag{3b}$$

The background field is known from the locations of the active electrodes. The data for the experiment may therefore be thought of as consisting of the voltage drops in the perturbational field at all adjacent electrodes, i.e.,

$$\delta u(1,\theta_{k+1}) - \delta u(1,\theta_k) = g_k - [U(1,\theta_{k+1}) - U(1,\theta_k)] =: \delta g_k \tag{4}$$

The problem is to determine $\delta\sigma(r,\theta)$ from knowledge of δg_k for a set of specified active electrode pairs i and j. For the backprojection method, we suppose that the active electrode pairs are

$$i \quad \text{and} \quad j = i + m, \quad \text{for} \quad i = 1,2,\ldots, n$$

with a fixed m, $1 \le m < n$. This way, we cycle through all electrodes pairs with separation m. By assumption, $\delta\sigma$ is only a perturbation. However, we do expect $\delta\sigma$ to achieve its largest values in a neighborhood of the crack.

One important element which greatly simplifies the backprojection algorithm is the fact we can write the background field U in closed form. Consider a single experiment in which current comes in at electrode i and exits at electrode $i+m$. We can find U corresponding to this applied current pattern using complex variables. Let (x,y) be the physical coordinates and form the complex variable $z = x + \mathbf{j}y$, where $\mathbf{j}$ denotes the imaginary unit. The active electrodes are at angles θ_i and θ_{i+m} on the unit circle; a point midway between these points is $\theta_* = (\theta_i + \theta_{i+m})/2$. These points correspond to the complex numbers

$$z_i = \exp \mathbf{j}\theta_i, \quad z_* = \exp \mathbf{j}\theta_*, \quad z_{i+m} = \exp \mathbf{j}\theta_{i+m}$$

We construct a fractional linear transformation $\zeta(\cdot)$ which takes the unit disk onto the unit disk and which maps these three points as follows[7]

$$\zeta(z_i) = 1, \qquad \zeta(z_*) = \mathbf{j}, \qquad \zeta(z_{i+m}) = -1$$

Finally, in the ζ-unit disk we define the complex function

$$W(\zeta) = \frac{1}{\pi}\log\frac{1+\zeta}{1-\zeta}$$

It is fairly easy to see that the background potential, U, is given by $U(x,y) = ReW(\zeta(z))$. Let V denote the harmonic conjugate to U, i.e., the function given by $V(x,y) = ImW(\zeta(z))$. Consider the conformal transformation $W(\zeta(z)) = U(x,y) + \mathbf{j}V(x,y)$. The unit disk $\{x^2 + y^2 \le 1\}$ is mapped onto the horizontal strip $\{|V| \le 1/2\}$ in the (U,V)-plane. The points corresponding to the electrode locations are mapped as follows

$$z = \exp \mathbf{j}\theta_i + \rightarrow W = \infty + \mathbf{j}\frac{1}{2}$$

$$z = \exp \mathbf{j}\theta_i - \rightarrow W = \infty - \mathbf{j}\frac{1}{2}$$

$$z = \exp \mathbf{j}\theta_{i+m} - \rightarrow W = -\infty + \mathbf{j}\frac{1}{2}$$

$$z = \exp \mathbf{j}\theta_{i+m} + \rightarrow W = -\infty - \mathbf{j}\frac{1}{2}$$

(see Fig. 2).

In (U,V) coordinates, the perturbational problem (3) becomes

$$\triangle \delta u = -\frac{\partial \delta\sigma}{\partial U} \quad \text{for} \quad |V| < \frac{1}{2} \tag{5a}$$

$$\left.\frac{\partial \delta u}{\partial V}\right|_{|V|=1/2} = 0 \tag{5b}$$

The electrodes, located in the z-plane at

$$z_k = \exp \mathbf{j}\theta_k, \quad k = 1\ldots n$$

have been mapped to locations along $|V| = 1/2$. The electrodes located on the counterclockwise arc from z_i to z_{i+m} have been mapped to $V = 1/2$. The electrodes located on the clockwise arc from z_i to z_{i+m} have been mapped to $V = -1/2$. Interpolation of the data in (4) provides an approximation to $\partial\delta u/\partial U$ along $|V| = 1/2$. We shall pretend that this approximation represents the exact derivative, i.e., we shall pretend that we have

$$\frac{\partial \delta u}{\partial U}(U, V = \pm 1/2) = S_{\pm}(U) \tag{6}$$

where $S_{\pm}(U)$ are calculated from the data of this single experiment (δg_k for $k = 1,\ldots,n$).

For a single experiment, it is now possible to construct a *consistent* conductivity perturbation $\delta\sigma$ which satisfies *both* the governing Eq. (5) and the data Eq. (6). Clearly, such a consistent conductivity perturbation, $\delta\sigma$, is not unique. To construct $\delta\sigma$, we choose δu to be of the form

$$\delta u(U,V) = S_+(U)h(V) + S_-(U)h(-V)$$

where $h(V)$ is chosen such that

$$h\left(\frac{1}{2}\right) = 1 \text{ and } h'\left(\frac{1}{2}\right) = h\left(-\frac{1}{2}\right) = h'\left(-\frac{1}{2}\right) = 0 \quad (7)$$

A most natural choice is to take h in the form of a cubic polynomial. The above δu clearly satisfies the Neumann boundary condition in (5). Inserting (7) in (5) we find the following formula for a consistent $\delta\sigma$

$$\delta\sigma(U,V) = -S'_+(U)h(V) - S'_-(U)h(-V) - \left[\int^U S_+(\tilde{U})d\tilde{U}\right]h''(V) - \left[\int^U S_-(\tilde{U})d\tilde{U}\right]h''(-V) \quad (8)$$

This image, obtained from the single experiment with input electrode at θ_i and output electrode at θ_{i+m}, may now, by the inverse of the transformation $z \to W(\zeta(z))$, be mapped back to the (x,y) coordinates; the result will be denoted

$$\delta\sigma^{(i)}(x,y)$$

The idea behind backprojection is to construct the desired conductivity image as a superposition of images obtained from different single experiments. After cycling through the n electrode pairs (θ_i,θ_{i+m}), the reconstructed conductivity perturbation is

$$\delta\sigma \approx \sum_{i=1}^{n} w^{(i)}(x,y)\delta\sigma^{(i)}(x,y)$$

where $w^{(i)}(x,y)$ are appropriate weight functions. If the weights were all chosen equal $(=1/n)$, then the sweep of the input (or the output) electrode would be uniform. This would result in a very distorted image near the boundary of the domain. Instead we choose

$$w^{(i)}(x,y) = \frac{d\rho}{d\theta}(\theta_i)$$

where we have used the notation θ for the variable input electrode location, and where the angle ρ is as shown in Fig. 3. With this choice the sweep of the arcs along which we "backproject," to obtain the image at the point $P(x,y)$, is uniform.

The backprojection procedure, for a fixed m, can algorithmicly be described as follows:

for $i = 1,\ldots,n$

1. Compute the maps $\zeta(z)$ and $W(\zeta)$
2. Interpolate boundary data δg_k to obtain $S_\pm(U)$
3. For the given point $P(x,y)$, find its image $W(\zeta(P))$
4. Compute the weight $w^{(i)}(x,y)$
5. Compute $\delta\sigma^{(i)}(x,y)$, using (8)
6. $\delta\sigma(x,y) \leftarrow \delta\sigma(x,y) + w^{(i)}(x,y)\delta\sigma^{(i)}(x,y)$

next i.

The backprojection method presented here is purely heuristic. However, in the special case of dipole sources, the backprojection algorithm may be justified as an inverse of a generalized Radon transform.[12] A dipole source is the limit that is obtained when the output electrode approaches the input electrode while the currents are scaled by the inverse of the electrode separation. An analogous theoretical investigation of the case with finite electrode separation is currently being carried out and will be reported elsewhere.

3. A CRACK FINDING ALGORITHM

We now give a brief description of an algorithm to determine certain parameters that characterize a crack (based on the same boundary measurements as before). We simplify the problem (reduce the number of parameters) by assuming that the crack is a line segment. In this case the crack is completely characterized by four parameters: the coordinates of the endpoints of the line segment.

Our algorithm is constructed to determine cracks that are perfectly conducting. By simple manipulations of the boundary data it may also be used to determine cracks that are perfectly insulating. As mentioned in Section 1, the conductivity distribution in the domain Ω (the unit disk) with a crack is formally given by

$$\sigma(x) = \begin{cases} \sigma_0 & \text{if } x \in \Omega\backslash\gamma \\ \infty & \text{if } x \in \gamma \end{cases}$$

where the line segment γ represents the crack. What this means more specifically is that the potential field, u, caused by sources at electrodes i and j, satisfies

$$\Delta u = 0 \quad \text{for } x \in \Omega\backslash\gamma \quad (9a)$$

$$u = \text{constant } x \in \gamma \quad (9b)$$

with the Neumann boundary condition, expressed in polar coordinates,

$$\sigma_0 \frac{\partial u}{\partial r}(1,\theta) = \chi(\theta,\theta_i) - \chi(\theta,\theta_j) \qquad (9c)$$

As before, we use the normalization $\int_{\partial\Omega} u = 0$. Suppose α and β represent the coordinates of the endpoints, so that the crack is given by

$$\gamma = \{x : x = \alpha + t(\beta - \alpha),\ 0 \le t \le 1\}$$

The data for a single experiment are the voltage drops across the adjacent electrodes

$$u(1,\theta_{k+1}) - u(1,\theta_k) = g_k \quad \text{for} \quad k = 1,\ldots,n$$

(we could also have worked with the data for $u - U$ as in the backprojection algorithm, indeed we do so in our later implementation). The problem is to find α and β, the coordinates of the endpoints of the crack γ. For convenience, we define a map F in terms of the relationship between the parameters of the crack, α and β, and the voltage drops, $u(1,\theta_{k+1}) - u(1,\theta_k)$ for $k = 1,\ldots,n$. In other words $F = (F_1,\ldots,F_n)$ is given by

$$F(\cdot,\cdot;\theta_i,\theta_j) : IR^4 \to IR^n \quad F_k(\alpha,\beta;\theta_i,\theta_j) := u(1,\theta_{k+1}) - u(1,\theta_k), \quad k = 1,\ldots,n$$

Notice that this map depends on the choice of the electrodes through which current is passed. To evaluate F for any given α and β, we solve (9) and evaluate the voltage drops $u(1,\theta_{k+1}) - u(1,\theta_k)$. The crack reconstruction problem can now be posed as follows: find α and β that satisfies

$$F_k(\alpha,\beta;\theta_i,\theta_j) = g_k \quad \text{for} \quad k = 1,\ldots,n$$

for an optimal pair of electrodes (θ_i,θ_j). The optimal electrode locations are also functions of α and β.

The outline of the computational strategy is:

0. Make an initial guess for α and β.

While $\|\delta\alpha\|^2 + \|\delta\beta\|^2 >$ tolerance:

1. Find an optimal pair of electrodes, θ_i and θ_j, for the current crack location.
2. Evaluate the functions $F_k(\alpha,\beta;\theta_i,\theta_j)$, $k = 1,\ldots,n$.
3. Measure voltage drop data g_k for $k = 1,\ldots,n$, using the above electrode locations.
4. Compute the residuals $g_k - F_k(\alpha,\beta;\theta_i,\theta_j)$, $k = 1,\ldots,n$.
5. Find increments $\delta\alpha$ and $\delta\beta$ based on the residuals.
6. Update $\alpha \leftarrow \alpha + \delta\alpha$, $\beta \leftarrow \beta + \delta\beta$.

We next provide some details of how the steps 1–5 are carried out.

Optimal Electrodes. The choice of the active pair of electrodes is very important for the success of the crack determination algorithm. Our algorithm relies on a strategy first presented in Ref. 13. We briefly describe this strategy below.

For some fixed α and β, we denote the angle between the line segment γ and the horizontal axis by ρ. We consider the functional

$$J(\theta_i,\theta_j) = \sum_{k=1}^{n} F_k(\alpha,\beta;\theta_i,\theta_j)\phi_k$$

for a particular choice of the constants ϕ_k, and we select θ_i and θ_j so as to make $\frac{d}{d\rho}J(\theta_i,\theta_j)$ as large as possible (in reality ϕ_k are also chosen to be functions of α and β). Please consult Ref. 13 for details.

This selection can be interpreted as one that makes the functional J maximally sensitive to small rotations (and small transverse translations) of the crack γ. Having F (or J) depend sensitively on γ is desirable because it leads to a large mismatch in the residual $g_k - F_k(\alpha,\beta;\theta_i,\theta_j)$ when the true crack is markedly different from the crack described by the current values of α and β. This is discussed in more detail in Ref. 13, where we also observed that this selection seems to generically create a field u whose equipotential curves are almost orthogonal to the crack γ. It turns out that the optimal electrode locations can be determined from the solution to an auxiliary elliptic boundary value problem. In our present implementation we use a boundary element method to find an approximate solution.

Evaluation of the Map F. To evaluate the map $F(\alpha,\beta;\theta_i,\theta_j)$, we need to solve the boundary value problem (9). In our present implementation we find an approximate solution to (9) by a boundary element method. A boundary element method is feasible and very efficient, since the medium is homogeneous except for the crack. We refer the reader to Ref. 5 for a detailed discussion of the implementation of a boundary element method for the (multiple) crack problem (see also Ref. 11).

Measurement of Voltage Drops. Once the optimal electrode locations are determined, we measure (rather: we extract from measurements) the voltage drops corresponding to the potential with current sources at these optimal locations. See the later section about the experimental setup for more details.

Increments for Updates. The scheme for updating the crack locations is based on the solution of a constrained linear least squares problem. Given the present values of α and β, and the optimal electrode locations θ_i and θ_j, we compute the Jacobian of the map F, i.e., we compute

$$\frac{\partial F_k}{\partial \alpha_m}(\alpha,\beta;\theta_i,\theta_j) \quad \text{and} \quad \frac{\partial F_k}{\partial \beta_m}(\alpha,\beta;\theta_i,\theta_j)$$
$$\text{for} \quad m = 1,2; \quad k = 1,\ldots,n$$

We seek to minimize the expression

$$\sum_{k=1}^{n} \left| \sum_{m=1}^{2} \frac{\partial F_k}{\partial \alpha_m} \delta\alpha_m + \sum_{m=1}^{2} \frac{\partial F_k}{\partial \beta_m} \delta\beta_m - (g_k - F_k) \right|^2$$

(with respect to $\delta\alpha$ and $\delta\beta$) subject to the bound

$$\|\delta\alpha\|^2 + \|\delta\beta\|^2 \leq \lambda^2$$

The number λ is chosen conservatively small to make the ultimate convergence of the algorithm less dependent on the initial guess. The minimization is reminiscent of the trust region method; one notable difference is that we change the electrode locations after each update of the crack. We keep the "trust radius" λ constant.

In the present implementation, the Jacobian was computed by a finite difference approximation. This involves solving four additional boundary value problems like (9). A boundary element method is again employed to obtain approximate solutions. For other possible ways of calculating the Jacobian see Refs. 13 and 5.

4. THE LABORATORY SETUP

We now briefly describe the laboratory experiments that were performed to generate "real" data in order to test the feasibility of Electrical Impedance Tomography.

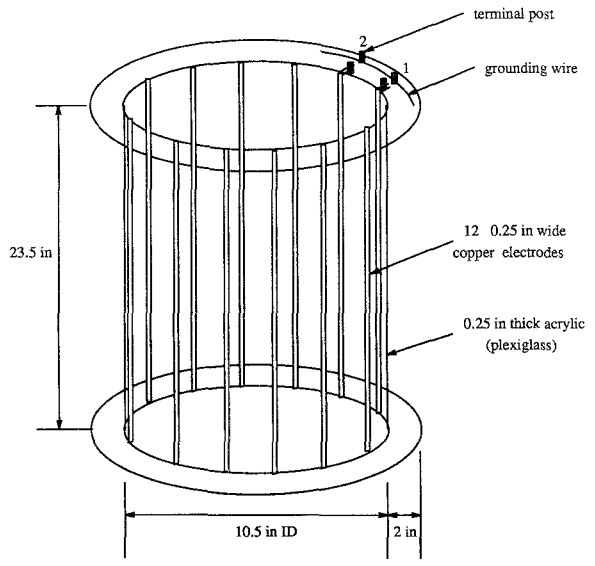

Fig. 4. The design of the tank.

A cylindrical tank with 12 electrodes was constructed. Measurements were performed using an automated data acquisition system consisting of a PC, an alternating current source, a digital voltmeter, a digital ammeter, and a switching network.

In the mathematical model for the problem, we have assumed that the voltage potential behaves like that of static direct current. We found that the use of a static (DC) current source was impractical in the actual experiments. The reason being that the use of a DC current source causes an electrolysis effect in the system. A consequence of the electrolysis is an alteration of the surface properties of the electrodes. Our method requires the collection of many measurements, and it is crucial that the properties of the system remain constant during the time it takes to collect these measurements. Therefore we use an AC source, operating at 1 kHz. This frequency is sufficiently low that the AC field may be thought of as a DC field times a harmonic modulation. The measured voltage drops for the AC field, up to a sign, gives the voltage drops for the DC field.

Figure 4 shows the lay-out of the tank. It is made of 0.25 inch thick clear acrylic (plexiglass), has an inside diameter of 10.5 inches and is 23.5 inches high. Attached to the inside surface of the cylinder are 12 vertical and equally spaced copper tape electrodes, each 0.25 inches wide and 0.001 inches thick.

At the top, each electrode strip is attached to a binding post. These binding posts are connected with wires to the data acquisition system. Next to the electrode binding posts is a second set of binding posts. The posts in the second set are all interconnected to form a common ground to which the shields for the data wires are connected. When the tank is filled with electrolyte (a slightly conducting water), the tank is believed to simulate a two-dimensional geometry as far as conductance between the electrodes is concerned.

A block diagram of the data acquisition system is shown in Fig. 5. It consists of an alternating current (AC) voltage source, two digital multimeters used as a voltmeter and an ammeter, a bank of relay cards, and a PC for control and data acquisition. The design concept of the system was to be able to apply a voltage drop across any two electrodes and then measure the voltage drop across any other two electrodes, including the ones to which voltage is applied. The drive, or input, current is measured with a digital ammeter connected in series with the source. To achieve this versatility, four relay switches are used at each tank electrode to connect either to a $+/-$ source, or to a $+/-$ voltmeter lead. A total of 48 relays are switched via an A-bus interface (Alpha Products) by the PC (HP Vectra). The PC also collects

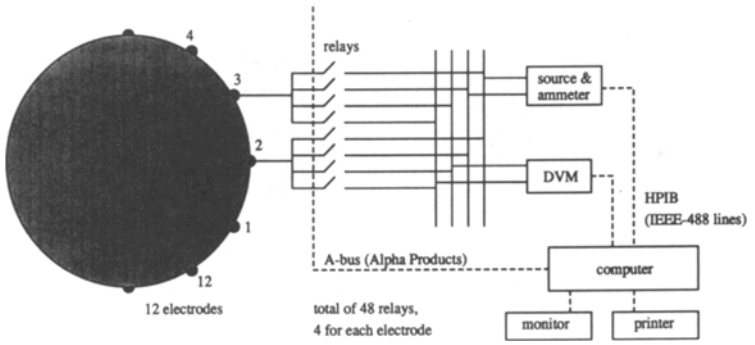

Fig. 5. Block diagram of the data acquisition system.

data via the IEEE-488 bus (Hewlett-Packard HP-IB) from the voltmeter and the ammeter.

The data acquisition software was written in BASIC and can be run in either manual or automatic mode. In the manual mode, the user specifies the active (source) electrode pair, and the measurement electrode pair. The measured voltage drop and the current are displayed on the monitor. This mode is used mostly for set-up and troubleshooting. The automatic mode collects data in the so-called "dipole" mode. Here a voltage drop is applied to a pair of adjacent electrodes, starting with electrodes 1 and 2, and voltage drops are measured across all the other adjacent electrodes. Voltage is then applied to the next pair of electrodes, and the process is repeated until voltage has been applied to all the electrodes. At each active electrode pair, current is also measured. Since we are using an AC source, only absolute voltage drops are readily measurable. The DC voltage field generated by a "dipole" source in the homogeneous tank has the property that all the voltage drops are of one sign except for the drop across the active electrodes (which is of the opposite sign). We added signs to our data by insisting that the same property hold. It is possible to build a system which can measure the voltage drops in phase so that the sign will also be available. This would eliminate the need for the above somewhat *ad hoc* approach.

The measured data are best displayed in the matrix form

$$\begin{bmatrix} V_2 - V_1 & V_3 - V_2 & \cdots & V_1 - V_{12} & I_{2,1} \\ V_2 - V_1 & V_3 - V_2 & \cdots & V_1 - V_{12} & I_{3,2} \\ \cdot & \cdot & & \cdot & \cdot \\ \cdot & \cdot & & \cdot & \cdot \\ V_2 - V_1 & V_3 - V_2 & \cdots & V_1 - V_{12} & I_{1,12} \end{bmatrix} \tag{10}$$

where V_i represents the voltage at electrode i, and $I_{j+1,j}$ represents the current flowing from electrode j to electrode $j + 1$. The order in which we cycle through the active electrode pairs is indicated by the indices in the last column of the matrix.

To make the measurements, the tank was first filled with distilled water. Then we added approximately a cup of tap water to produce an impedance of about 1 kΩ. The applied voltage drop were set to about 5 V (rms), 1 kHz sinusoidal.

The tank with the electrolyte simulates a homogeneous medium. Crack discontinuities are introduced by placing metal strips of various widths vertically in the tank. In the results presented in the next section, only a single flat strip was used. The data can just as easily be obtained for multiple strips, flat and curved.

5. RECONSTRUCTION FROM EXPERIMENTAL DATA

We now present the results we obtained by applying the algorithms discussed in Sections 2 and 3 to experimental data collected by the system described in Section 4.

The data collected correspond to the "dipole" mode. That is, we applied a fixed voltage drop across an adjacent pair of electrodes to generate a voltage potential in the tank. Then we measured the voltage drops across all other electrode pairs as well as the current flowing across the electrodes at which voltage is applied. Our data set is most conveniently viewed as the matrix (10) in the previous section. We found the currents to be of nearly the same size.

In order to use the measured data for reconstruction, we need to know the value of σ_0. Alternatively, we need to know the scaling factor that transforms the data into

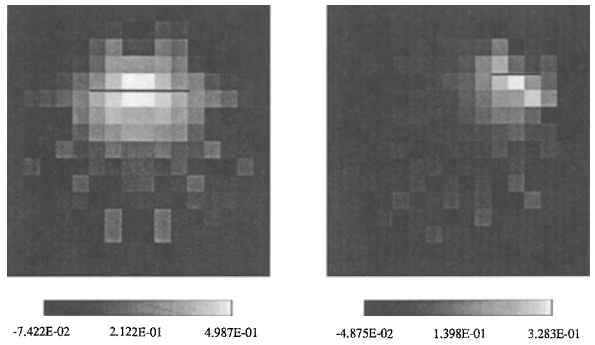

Fig. 6. The images obtained by applying the backprojection algorithm on the measured data. The exact locations of the cracks are shown for reference.

data for a tank corresponding to $\sigma_0 = 1$ and unit applied current. To obtain this scaling factor we computed the voltage drop across the active (adjacent) electrodes for a homogeneous tank with $\sigma_0 = 1$ and unit applied current. This number turned out to be 0.067514. We scaled all the voltage drop entries of the data matrix by the factor $0.067514/(V_2 - V_1)$ (that is the $V_2 - V_1$ coming from the first row of the data matrix). The scaled voltage data are now well approximated by our mathematical model corresponding to $\sigma_0 = 1$ and unit applied current. A particularly good fit was found using an electrode width of $h = 4^0$.

For the backprojection algorithm, the data we need are the difference in the voltage drops between the inhomogeneous experiment and the homogeneous one. Subtraction has the desirable property that some of the irregularities in the data set could be eliminated, since we expect the same irregularities to be present whether there is a crack or not. We will also use the difference as data for our crack finding algorithm. This requires only a small modification of the algorithm described before. In a real application, we may not always have the measured data for a homogeneous specimen. In that case, knowledge of σ_0 must be available to numerically generate the homogeneous data.

Recall that the crack finding algorithm determines best electrodes across which a voltage drop should be applied at each iteration. We have not measured data corresponding to these electrodes, rather the data we have measured correspond to dipole sources. As a consequence, some simple processing is needed to extract the required data from the matrix above. Note that all possible independent information has been recorded in the data matrix. To obtain the data needed, we just have to take appropriate linear combinations of the rows of the data matrix.

We shall report on the results of two experiments. To generate the data required for the two experiments, we make three sets of measurements. The first set of measurements is done with a homogeneous tank (no crack). The second and the third set of measurements are done with a crack inside the tank. As mentioned previously, a crack is simulated by immersing a metal strip vertically at some location. For the second set of measurements, we immersed a 4-inch strip to simulate a crack whose endpoints are

$$(-0.38, 0.38) \quad \text{and} \quad (0.38, 0.38)$$

(in units of the cross section radius). The third set of measurements involve a 2-inch strip simulating a crack with endpoints at

$$(0.24, 0.50) \quad \text{and} \quad (0.62, 0.50)$$

The collected data are normalized in the way we mentioned above. We compute the differences by subtracting the data matrix corresponding to the homogeneous tank from the second and the third data matrices we collected. The two datasets are now ready for the reconstruction algorithms.

The results of the backprojection algorithm applied to the datasets are shown in Figs. 6a and b. In each figure, we superposed the actual locations of the crack for reference. In viewing these results, we must keep in mind that there is a substantial amount of noise in the data in the form of measurement errors, as well as some modeling errors. These results do however indicate that the data are sufficiently accurate for the backprojection algorithm to reconstruct a rough image of the cracks. However, the images are too blurry to give good estimates, for instance of the crack sizes. In general, even with perfect data, this is probably the best we can hope for with the backprojection algorithm.[2,3,12]

The result of application of the crack finding algorithm on the experimental data gave a more satisfactory estimate of the exact locations and lengths of the cracks. In applying it to the first data set, we took the initial guess to be a crack whose endpoints are $(-0.5, 0)$ and $(0.5,0)$. The algorithm converged in four iterations. The result of this calculation is summarized in Figs. 7a–c. In Fig. 7a, we give a comparison of the measured data with the computed data corresponding to the initial guess. The active electrodes are electrodes 6 and 12. Shown in Fig. 7b is a comparison of the measured data with the computed data corresponding to the solution obtained by the algorithm. At convergence of the iterative method, current is flowing from electrode

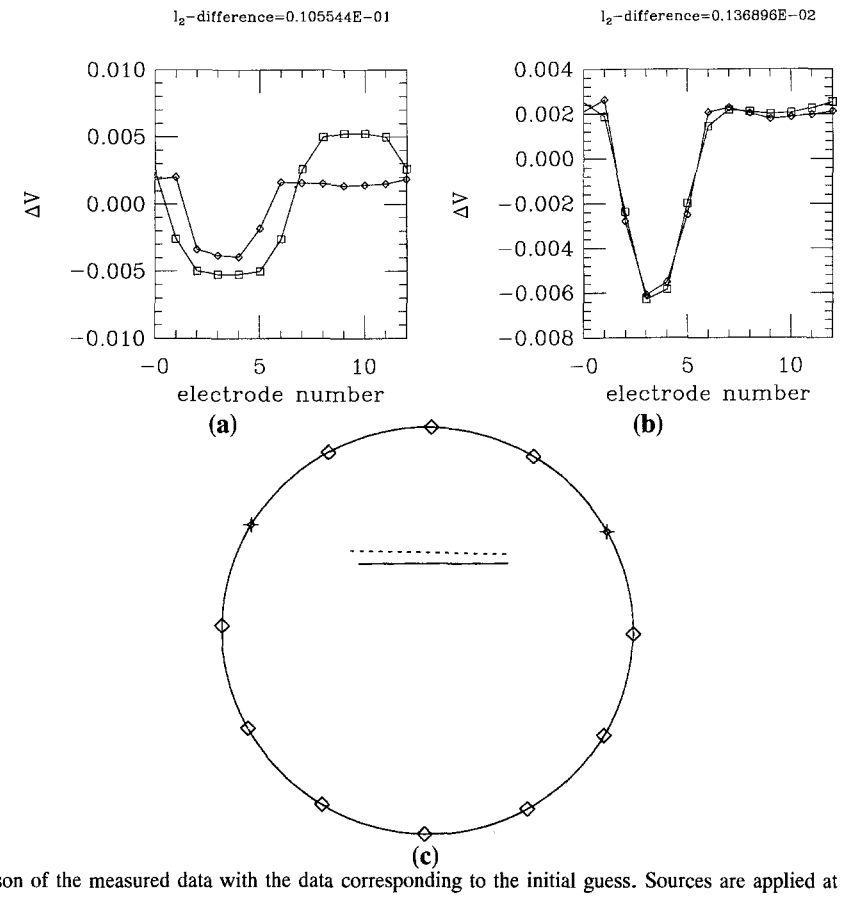

Fig. 7. (a) The comparison of the measured data with the data corresponding to the initial guess. Sources are applied at electrodes 6 and 12. (b) The comparison of the measured data with the data corresponding to the crack reconstructed by our algorithm. Sources are applied at electrodes 1 and 5. In both figures, the measured data are shown in ◇, the computed data are shown in □. (c) A comparison of the actual crack with the crack reconstructed by our algorithm. The active electrodes are indicated by the symbol ⊕. The algorithm took four iterations to reconstruct the crack shown in solid line. The actual crack is shown in dashes.

1 to electrode 5. Figure 7c gives a comparison of the actual crack (shown in dashes) with the crack found by the algorithm. The active electrodes at convergence are indicated by use of the symbol ⊕. The reconstruction yielded a crack whose endpoints are (−0.3402, 0.3173) and (0.3885, 0.3341).

An initial guess in the form of a crack with endpoints at (0,0) and (0.5,0) was used when applying the algorithm to the second dataset. The result of this calculation is displayed in Figs. 8a–c. In Fig. 8a the measured dataset is compared to the computed dataset corresponding to the initial guess. At this stage, current is applied at electrodes 6 and 12. In Fig. 8b, we compare the measured dataset with the computed dataset corresponding to the crack reconstructed by our algorithm (convergence occurs after five steps). At convergence, sources are applied at electrodes 1 and 4 as indicated in Fig. 8c. A comparison of the actual location of the crack with the reconstructed crack is made in Fig. 8c. The reconstruction yielded a crack whose endpoints are (0.1964, 0.4666) and (0.5703, 0.4773).

Based on these results, we propose an inspection strategy which consists of first using the backprojection algorithm to detect the presence of a crack. If a crack is detected, we use the result from the backprojection algorithm to obtain an initial guess for the crack finding algorithm. These initial findings seem to indicate that Electrical Impedance Tomography may prove to be a promising nondestructive evaluation technique for certain applications.

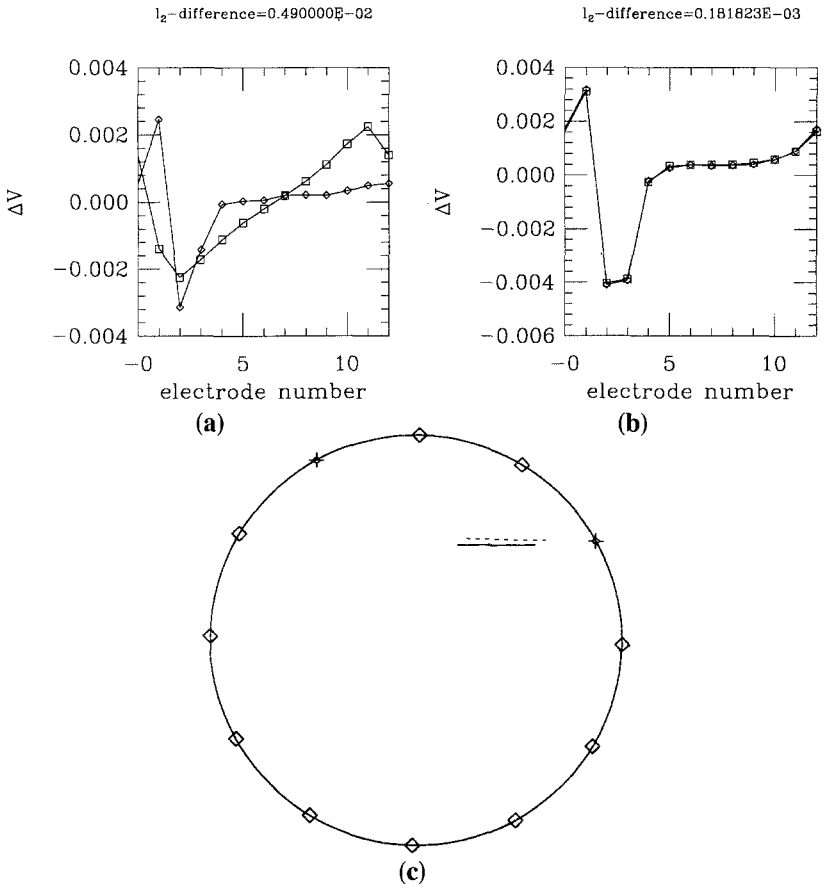

Fig. 8. (a) The comparison of the measured data with the data corresponding to the initial guess. Sources are applied at electrodes 6 and 12. (b) The comparison of the measured data with the data corresponding to the crack found by our method. Sources are applied at electrodes 1 and 4. In both figures, the measured data are shown in ◇, the computed data are shown in □. (c) A comparison of the actual crack with the crack reconstructed by the algorithm. The active electrodes are indicated by the symbol +. The algorithm took five iterations to reconstruct the crack shown in solid line. The actual crack is shown in dashes.

ACKNOWLEDGMENT

The interdisciplinary collaboration which constitutes part of this work was greatly facilitated by National Science Foundation grant DMS-89-12593. Fadil Santosa is partially supported by NSF grant DMS-90-11076 and AFOSR contract 81-NM-875. Michael Vogelius is partially supported by NSF grant DMS-89-02532 and AFOSR contract 89-NM-605.

REFERENCES

1. S. Andrieux and A. Ben Abda. Identification de fissure planes par une donnée de bord unique: un procédé direct de localisation et identification, *C.R. Acad. Sci Paris* t. **315** (Série I):1323–1328 (1992).
2. D. Barber and B. Brown. Recent developments in applied potential tomography—APT, in *Information Processing in Medical Imaging*, S. Bacharach, ed. (Nijhoff, Amsterdam, 1986), pp. 106–121.
3. D. Barber and B. Brown. Progress in electrical impedance tomography, in *Inverse Problems in Partial Differential Equations*, D. Colton *et al.*, eds. (SIAM Publications, Philadelphia), pp. 151–164 (1990).
4. K. Bryan and M. Vogelius. A uniqueness result concerning the identification of a collection of cracks from finitely many electrostatic boundary measurements, *SIAM J. Math. Anal.* **23**:950–958 (1992).
5. K. Bryan and M. Vogelius. A computational algorithm for crack determination. The multiple crack case. *Int. J. Eng. Sci.* (to appear).
6. M. Cheney, D. Isaacson, J. Newell, S. Simske, and J. Goble. NOSER: An algorithm for solving the inverse conductivity problem. *Int. J. Imaging Syst. and Technol.* **22**:66–75 (1990).
7. R. V. Churchill and J. W. Brown. *Complex Variables and Applications* (McGraw-Hill Book Co., New York, 1984).
8. M. Eggleston, R. Schwabe, D. Isaacson, and L. Coffin. The Application of Electric Current Computed Tomography to Defect

Imaging in Metals, GE Research and Development Center Technical Information Series 89CRD158, 1989.
9. A. Friedman and M. Vogelius. Determining cracks by boundary measurements, *Ind. Univ. Math. J.* **38**:527–556 (1989).
10. R. Halmshaw, *Non-Destructive Testing* (Edward Arnold, London, 1987).
11. N. Nishimura and S. Kobayashi. A boundary integral equation method for an inverse problem related to crack detection, *Int. J. Num. Meth. Eng.* **32**:1371–1387 (1991).
12. F. Santosa and M. Vogelius. A backprojection algorithm for electrical impedance imaging, *SIAM J. Appl. Math.* **50**:216–243 (1990).
13. F. Santosa and M. Vogelius. A computational algorithm to determine cracks from electrostatic boundary measurements, *Int. J. Eng. Sci.* **29**:917–937 (1991).